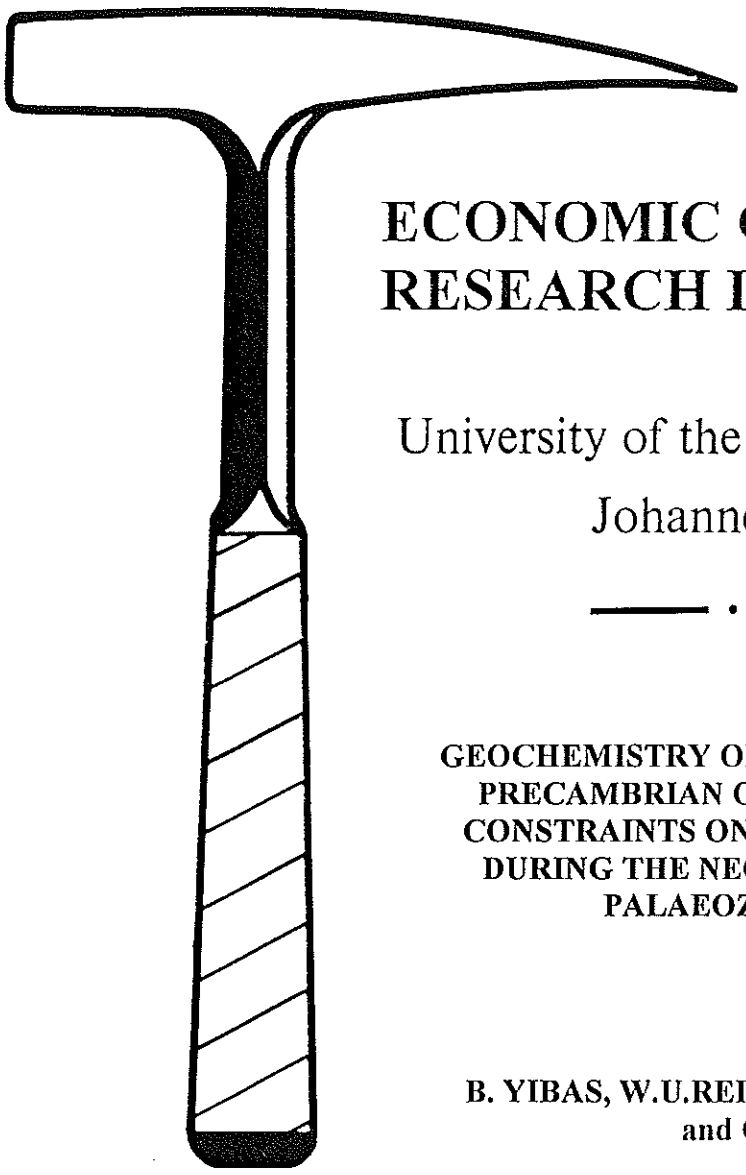

ECONOMIC GEOLOGY RESEARCH INSTITUTE

University of the Witwatersrand

Johannesburg

GEOCHEMISTRY OF THE GRANITOIDS IN THE PRECAMBRIAN OF SOUTHERN ETHIOPIA: CONSTRAINTS ON THE TECTONIC REGIME DURING THE NEOPROTEROZOIC-EARLY PALAEOZOIC (900-500 Ma)

B. YIBAS, W.U.REIMOLD, C.R.ANHAEUSSER and C.KOEBERL

INFORMATION CIRCULAR No.350

UNIVERSITY OF THE WITWATERSRAND
JOHANNESBURG

GEOCHEMISTRY OF THE GRANITOIDS IN THE PRECAMBRIAN OF SOUTHERN ETHIOPIA: CONSTRAINTS ON THE TECTONIC REGIME DURING THE NEOPROTEROZOIC-EARLY PALAEOZOIC (900-500 Ma)

by

B. YIBAS[1], W.U.REIMOLD[1*], C.R. ANHAEUSSER[2] AND C. KOEBERL[3]

([1]Geology Department, University of the Witwatersrand, Private Bag 3, Wits 2050, Johannesburg, South Africa

[2]Economic Geology Research Institute, Geology Department, University of the Witwatersrand, Private Bag 3, Wits 2050, Johannesburg, South Africa

[3]Institute of Geochemistry, University of Vienna, Althan Str.14, A-1090 Vienna, Austria

**Corresponding Author)*

**ECONOMIC GEOLOGY RESEARCH INSTITUTE
INFORMATION CIRCULAR No.350**

December, 2000

GEOCHEMISTRY OF THE GRANITOIDS IN THE PRECAMBRIAN OF SOUTHERN ETHIOPIA: CONSTRAINTS ON THE TECTONIC REGIME DURING THE NEOPROTEROZOIC-EARLY PALAEOZOIC (900-500 Ma)

ABSTRACT

The granitoids of southern Ethiopia include gneisses and undeformed granites. They vary compositionally from granites to diorites, with the dioritic rocks being less abundant. Most of these granitoids consistently show metaluminous, peralkaline and calcic affinities similar to Cordilleran and other young fold-belt granites. Average chondrite-normalised REE data of most samples are comparable to those of Late Proterozoic and younger granites in the Northeastern Desert of Egypt and the Red Sea Hills in Sudan. The HREE fractionation patterns of most samples show similarities to granitoids from continental margin settings (viz., intermediate calc-alkaline rocks) and often have $[Tb/Yb]_N>1$, which is rare or absent in island-arc granitoids. Spider diagrams indicate enrichment of the most incompatible elements (Rb, Th and Ba) relative to REEs, a regular decrease of the enrichment factor with increasing compatibility of the elements, and strong negative Nb, P, Sr and Ti anomalies. These features are characteristic of subduction-related magmas and are noted for most East African Orogen granitoids.

Tectonic discriminant diagrams classify these granitoids into volcanic-arc and within-plate granitoids. The within-plate granitoids are restricted to the field of attenuated continental crust and anomalous oceanic-ridge granites, and have affinity with A2-type granitoids that include magmas derived from continental crust or underplated crust that has been through a cycle of continent-continent collision or island-arc magmatism.

The granitoids of the Precambrian of southern Ethiopia show similar geochemical characteristics to granitoids from western Ethiopia, but differ from those of northern Ethiopia where within-plate granitoids are absent and volcanic-arc I-type granitoids are dominant. They do, however, have similar emplacement ages. The geochemical interpretation for the granitoids of southern Ethiopia shows alternation of within-plate and volcanic-arc granitic magmatism suggesting repeated compressional and extensional tectonic regimes during the East African Orogen (900-500Ma).

oOo

GEOCHEMISTRY OF THE GRANITOIDS IN THE PRECAMBRIAN OF SOUTHERN ETHIOPIA: CONSTRAINTS ON THE TECTONIC REGIME DURING THE NEOPROTEROZOIC-EARLY PALAEOZOIC (900-500 Ma)

CONTENTS

oOo

Published by the Economic Geology Research Institute
Department of Geology
University of the Witwatersrand
1 Jan Smuts Avenue
Johannesburg 2001

www.wits.ac.za/egru

ISBN 1-86838-296-6

GEOCHEMISTRY OF THE GRANITOIDS IN THE PRECAMBRIAN OF SOUTHERN ETHIOPIA: CONSTRAINTS ON THE TECTONIC REGIME DURING THE NEOPROTEROZOIC-EARLY PALAEOZOIC (900-500 Ma)

INTRODUCTION

The study area of over 88000 km^2 is situated in southern Ethiopia (Fig. 1). It occupies a unique position in the East African Orogen in that it covers the northern part of the Mozambique Belt and the southern part of the Arabian Nubian Shield.

The results presented here form part of a comprehensive regional study, which involved the production of geological and structural maps, and the acquisition of new petrographic, geochronological and geochemical data (Yibas, 2000). The Precambrian of southern Ethiopia comprises two distinct tectonostratigraphic terranes, which are separated by repeatedly reactivated structural zones. These terranes are referred to as: (1) the granite-gneiss terrane; and (2) ophiolitic fold and thrust belts (Yibas, 2000; Yibas et al., 2000a; Fig. 1b).

The granite-gneiss terrane consists of para- and ortho-quartzofeldspathic gneisses and granitoids intercalated with amphibolites, sillimanite-kyanite-bearing schists, and marbles. The paragneisses show lithological similarities with gneisses from northern Kenya that were derived from sediments that filled the Kenyan sector of the "Mozambique Belt basin" during the period 1200 to 820 Ma (Key et al., 1989). The granitoid rocks in the study area vary from granitic gneisses to undeformed granites and range compositionally from diorites to granites (cf. below). The ophiolitic fold and thrust belts are composed of mafic, ultramafic and metasedimentary rocks in various proportions. Felsic volcanic rocks are virtually absent in these belts. The mafic rocks comprise massive amphibolites, amphibole schists, amphibole-chlorite schists and metagabbros. Amphibolites and amphibole schists are the dominant lithologies. Undeformed granitoids are also not uncommon in the ophiolitic fold and thrust belts (Yibas, 2000).

Based on field relationships (structure, petrography, texture, and contact relationships with adjacent lithologies), the granitoids of southern Ethiopia can be broadly classified into granitoid gneisses, deformed granitoids and undeformed (post-tectonic) granitoids (Yibas et al., 2000a, b).

Granitoid Gneisses

The locations of the major granitoid gneisses in southern Ethiopia are shown in Figure 1b. These include the Yabello granitic gneiss (1, Fig. 1b), the Finchaa granitic gneiss (2), the Burji granitic gneiss (3), the Sodigga granitic gneiss (6), the Mega-Hidilola granitic gneiss (7), the Sololo granitic gneiss (8), the Raro-Kakisa-El Gof granitic gneiss (9) and the Sebeto tonalitic gneiss (10) (Yibas et al., 2000a). In most cases, these granitoids show strong deformational fabric, such as gneissic banding.

Deformed Granitoids

Examples of the deformed granitoids are also shown in Figure 1b and include the Gariboro and Burjiji granitoids (11), Bulbul mylonitic diorite (18), and the Moyale (4) and Meleka

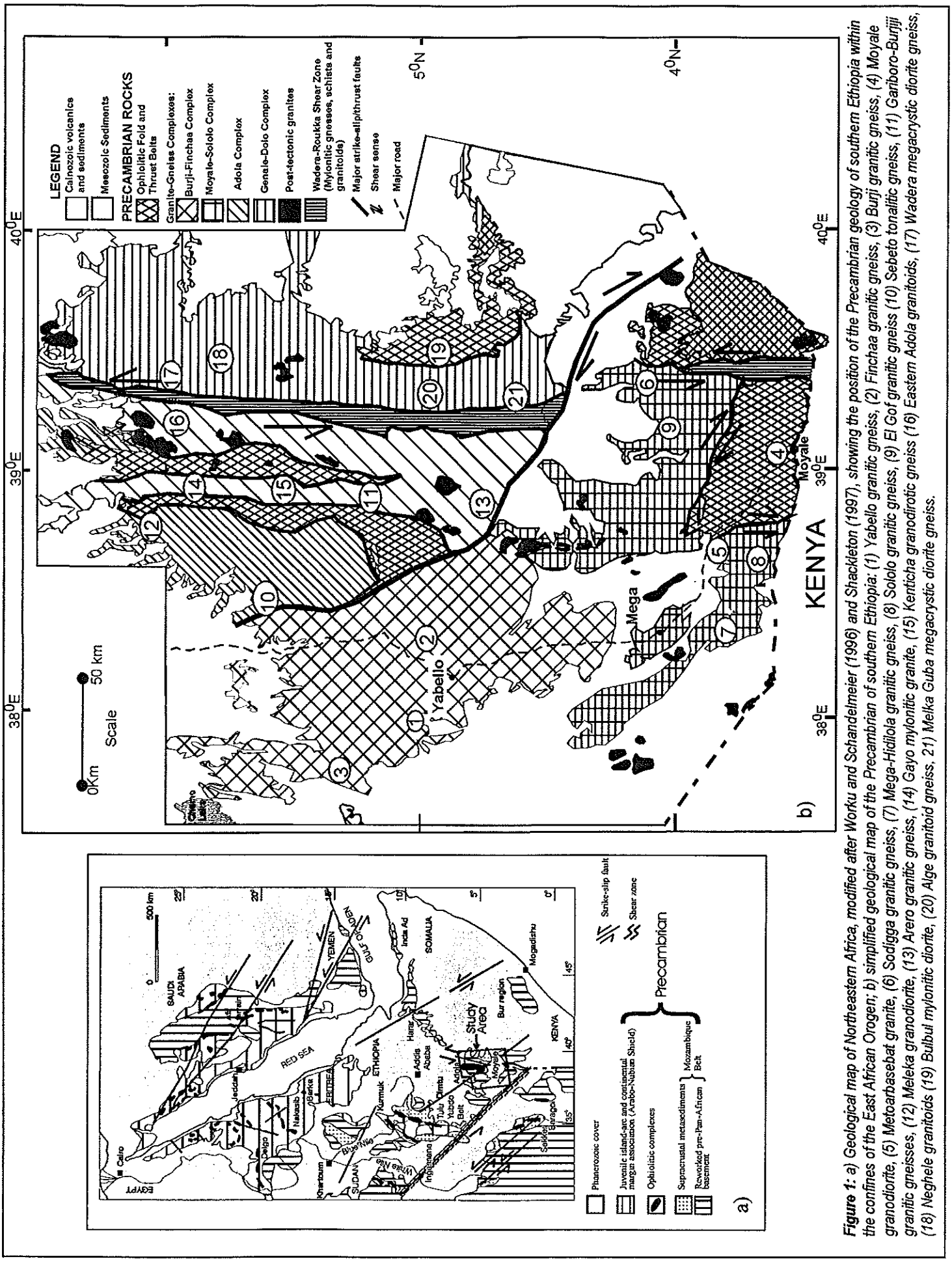

Figure 1: *a) Geological map of Northeastern Africa, modified after Worku and Schandelmeier (1996) and Shackleton (1997), showing the position of the Precambrian geology of southern Ethiopia within the confines of the East African Orogen; b) simplified geological map of the Precambrian of southern Ethiopia: (1) Yabello granitic gneiss, (2) Finchaa granitic gneiss, (3) Burji granitic gneiss, (4) Moyale granodiorite, (5) Metoarbassebat granite, (6) Sodigga granitic gneiss, (7) Mega-Hidilola granitic gneiss, (8) Sololo granitic gneiss, (9) El Gof granitic gneiss (10) Sebeto tonalitic gneiss, (11) Garlboro-Burjiji granitic gneisses, (12) Meleka granodiorite, (13) Arero granitic gneiss, (14) Gayo mylonitic granite, (15) Kenticha granodirotic gneiss (16) Eastern Adola granitoids, (17) Wadera megacrystic diorite gneiss, (18) Neghele granitoids (19) Bulbul mylonitic diorite, (20) Alge granitoid gneiss, 21) Melka Guba megacrystic diorite gneiss.*

(12) granodiorites. These rocks are often foliated, in places gneissose, and form elongated bodies parallel to the regional, mainly N-S trending foliation.

Late- to Post-tectonic (Undeformed) Granitoids

Most of the granites representing the final phase of granitic magmatism in southern Ethiopia are intrusive into the quartzofeldspathic and granitoid gneisses. Their contact relationships with the country rocks, where exposed, are sharp, steep and discordant to the regional N-S trending foliations. The size of these granitic bodies is variable, but when compared to the other suites of granites, they are generally smaller.

A number of samples from the different granitoids were dated using SHRIMP and $^{40}Ar/^{39}Ar$ laser-probe dating techniques (Yibas, 2000; Yibas et al., 2000a). The ages obtained, coupled with available field data, led to the classification of these granitoids into seven generations. These, in descending order of age, include: Gt1 (>850 Ma); Gt2 (800-770 Ma); Gt3 (770-720 Ma); Gt4 (720-700 Ma); Gt5 (700-600 Ma); Gt6 (580-550 Ma); and Gt7 (550-500 Ma) (Yibas, 2000; Yibas et al., 2000b). The period 550 to 500 Ma (Gt7) is marked by emplacement of late- to post-tectonic and post-orogenic granitoids, such as the Metoarbasebat granite (5 in Fig. 1b). Although the magmatic ages obtained from SHRIMP zircon dating range from 880 to 526 Ma, the $^{40}Ar/^{39}Ar$ ages for all these samples are younger that 550 Ma. This suggests that the Gt7 period represents the latest tectonothermal event (Yibas et al., 2000b).

In this paper, geochemical characterisation and classification of the quartzofeldspathic gneisses and granitoids will be presented to decipher the tectonic evolution during the Neoproterozoic-Early Palaeozoic (900-500 Ma) period of the southern Ethiopian part of the East African Orogen.

GEOCHEMISTRY

Methodology

About 130 samples were analysed for major, minor, and trace elements. Sample preparation was carried out at the Department of Geology, University of the Witwatersrand, Johannesburg, and in the Central Laboratory of the Ethiopian Institute of the Geological Surveys, Addis Ababa. Complex rock units such as migmatites and those with lit-par-lit structures were excluded. The samples were milled using chrome-steel discs in a rotary mill. Major and trace elements were analysed by X-ray fluorescence spectrometry (XRF) on fused glass discs and powder pellets in the Geology Department at the University of the Witwatersrand, Johannesburg. Details of XRF analysis and information regarding precision and accuracy can be obtained from Reimold et al. (1994). Trace elements, including REE, were determined by instrumental neutron activation analysis (INAA), following the methods described in Koeberl (1993), at the University of Vienna, Austria, and by inductively coupled plasma mass spectrometry (ICP-MS) at the Anglo American Research Laboratory, Johannesburg. Data tables can be obtained from the first author upon request.

General Geochemical Characteristics

Although most major and trace elements may be mobile during high-grade metamorphism, the use of these elements in relation to the mineralogical and overall chemical composition of rocks can be useful in deciphering their protolith types and tectonic setting. However, it

is invaluable to test how much of the original chemistry of a rock has been affected by alteration and metamorphism. Scattered trends on variation diagrams may be useful indicators of element mobility, although chemical alteration can sometimes produce systematic changes that mimic other processes such as crystal fractionation. It is essential, therefore, to demonstrate that the element concentrations are undisturbed by hydrothermal alteration or metamorphism before inferences can be made about the petrogenesis of a given rock suite (Rollinson, 1993).

The suites of quartzofeldspathic and granitoid gneisses of this study are indistinguishable in terms of their SiO_2 concentrations, which range from 63 to 85 wt%. They exhibit high alkali element (K_2O+Na_2O) contents (8-13 wt%), K_2O/Na_2O ratios of less than unity (as low as 0.16), and high concentrations of $Fe_2O_3^T$ (total iron as Fe_2O_3), TiO_2, Na_2O, MnO, MgO and Al_2O_3. SiO_2 in the granitoids and quartzofeldspathic gneisses from the Adola granite-gneiss complex ranges from about 63.8 to 77 wt%, with only three out of thirty samples having $SiO_2 < 70$ wt%. The SiO_2 concentrations in the quartzofeldspathic and granitoid gneisses from the Genale-Dolo granite-gneiss complex range from 59 to 78 wt%, with the majority of samples having >68 wt% SiO_2. SiO_2 abundance in the granitoids and quartzofeldspathic gneisses from the Moyale-Sololo granite-gneiss complex ranges from 60.6 to 77 wt%.

Protoliths of Quartzofeldspathic Gneisses

In Precambrian terrains, like that of southern Ethiopia, where the rocks have been subjected to high-grade metamorphism and polyphase deformation, one of the critical questions concerns the nature of the protoliths of quartzofeldspathic gneisses. A variety of chemical discrimination techniques have been proposed to distinguish quartzofeldspathic gneisses derived from igneous or sedimentary protoliths. Shaw (1972) used discrimination techniques based on major element composition and produced discrimination functions ($DF=10.44 -0.21\ SiO_2 - 0.32\ Fe_2O_3^T - 0.98\ MgO + 0.55\ CaO + 1.46Na_2O + 0.54\ K_2O$) for the distinction of sedimentary and igneous protoliths. Discrimination values (DF) > 0 indicate a probable igneous origin, whereas values < 0 indicate a sedimentary origin. This technique has been employed for a variety of gneissic suites and proved to be useful (e.g., Munyanyiwa et al., 1997). A chemical index of alteration (CIA), developed by Nesbitt and Young (1982), was also found to be useful to discriminate between gneisses of sedimentary and igneous parentage (e.g., Carl, 1988; Munyanyiwa et al., 1997). Unaltered granites and granodiorites have values of 0.44-0.55, whereas average values for shales are between 0.70 and 0.75 (Nesbitt and Young, 1982). Other discrimination diagrams useful for determining the parentage of quartzofeldspathic gneisses were developed, for example, by Van de Kamp and Beakhouse (1979). Most samples of this study have CIA values that are uniformly low (0.52-0.62) and are characterised by very high DF values that indicate igneous protoliths. The $(Na_2O+CaO)-Al_2O_3-K_2O$ diagram (not shown) of Nesbitt and Young (1984, 1989) and the QFM (quartz-feldspar-mafic minerals) diagram of Van de Kamp and Beakhouse (1979) support the interpretation that most of the quartzofeldspathic gneisses are of felsic igneous origin. As shown in Figure 2, only six samples fall into the arkosic field, which also show DF values <0. This is further supported by the P_2O_5/TiO_2 vs. Mg/CaO and Zr/TiO_2 versus Ni discrimination technique (after Rollinson, 1993), which shows that most of the samples exhibit very high Zr/TiO_2 ratios (up to 1300) for low Ni values (>50 ppm), again suggesting dominance of igneous parentage. Field and petrographic observations showed that most of the quartzofeldspathic gneisses sampled,

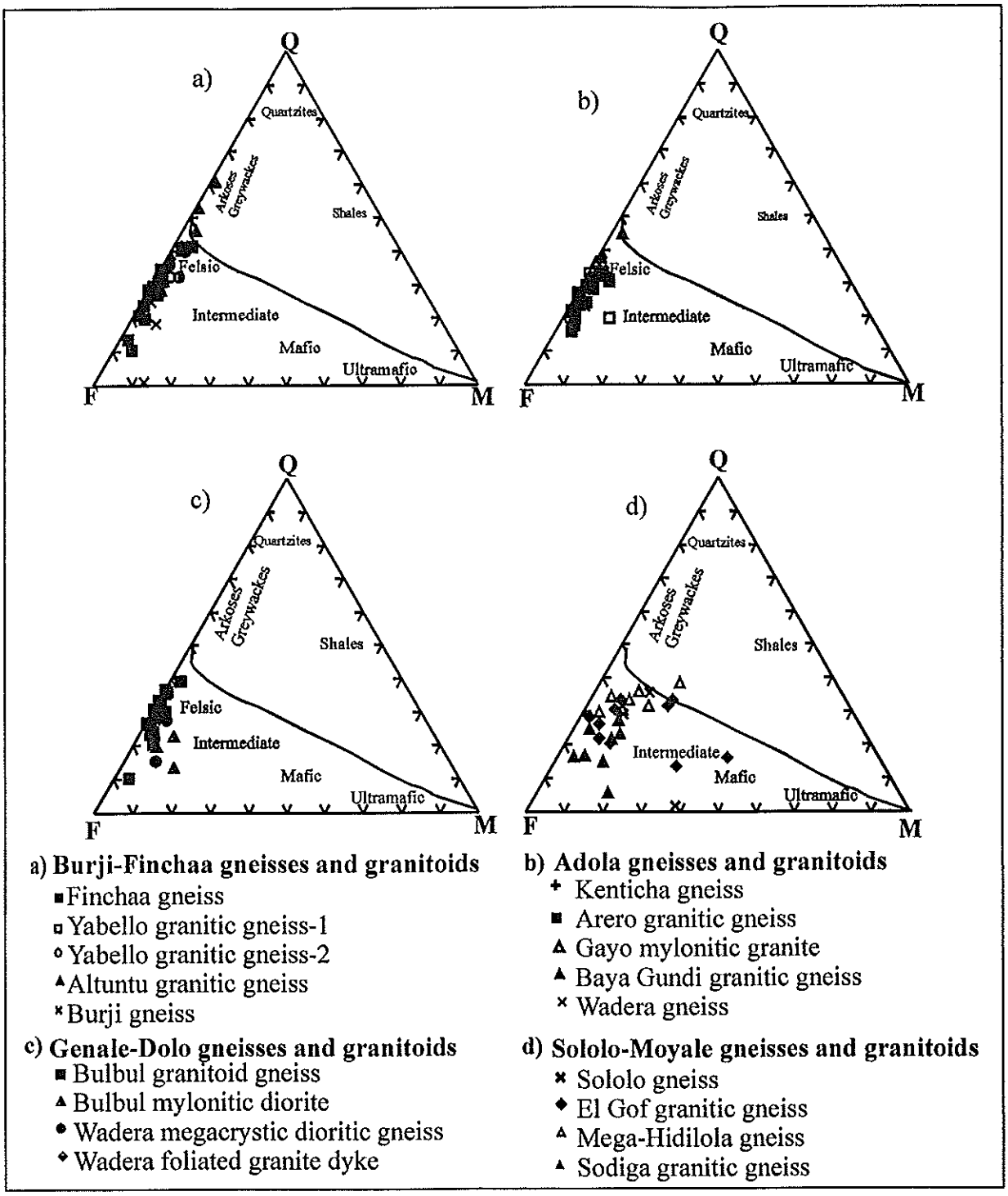

Figure 2: Discrimination diagrams of gneisses of sedimentary and igneous origin using quartz (Q), feldspar (F), and ferromagneisan minerals (M) (after Van de Kamp and Beakhouse, 1979).

display textural and mineralogical evidence of igneous parentage (Yibas, 2000) - consistent with these geochemical results.

Rock Classification and Designation

It is important to classify the rocks by chemical criteria (Irvine and Baragar, 1971) according to recognised international rock nomenclature, to compliment the field and

petrographic data and to allow meaningful comparison of a given rock suite with rock suites of similar chemical affinity from elsewhere. Because field and petrographic characteristics of the quartzofeldspathic gneisses, coupled with preliminary assessment of their protolith types, suggest that their protoliths are dominated by intrusive igneous rocks (Fig. 2), these data have been plotted on intrusive igneous rock discrimination diagrams. Trends on various discrimination diagrams suggest that these rocks are dominated by highly evolved monzogranites, with subordinate monzodiorites, granodiorites, and tonalites (Figs. 3, 4). These geochemical characteristics are supported by petrographic observations which showed that biotite and hornblende are the typical mafic components (Yibas, 2000).

Rare Earth Elements (REE)

Rare earth elements (REE) are regarded as amongst the least soluble trace elements and are relatively immobile during low-grade metamorphism, weathering, and hydrothermal alteration. The REE pattern of an igneous rock is controlled by the REE chemistry of its source and crystal-melt equilibria during its evolution, either during partial melting in the source region or during subsequent crystal fractionation (Rollinson, 1993). The usefulness of the REEs in petrogenetic studies lies in their ability to act as cohesive geochemical entities (Hanson, 1978). The REE data for the major granitoids of the different complexes are plotted in Figure 5.

Burji-Finchaa Granitoids

The Finchaa granitic gneiss (2 in Fig.1) shows relatively high chondrite-normalised values, with moderate to strong negative Eu anomalies ($Eu/Eu^* = 0.08$-0.16), is LREE enriched ($[La/Sm]_N = 2.45$-6.35), and has flat HREE ($[Tb/Yb]_N = 0.97$-1.27) and less fractionated REE patterns ($(La/Yb)_N = 3.33$-8.43, with the highest being 12.68). Three subgroups can be recognised based on: (1) $[La/Yb]_N$ (4, 7.16, and 18.2), which is a measure of the degree of REE fractionation; (2) $[La/Sm]_N$ (2.5, 4.75 and 6.35), which is a measure of the degree of LREE enrichment; and (3) relative HREE abundances. These three subgroups are similar with respect to their HREE fractionation $[Tb/Yb]_N$ (close to unity for all subgroups). A single sample from the Finchaa granitic gneiss shows a distinctly different pattern with a lower REE abundance than the other samples, moderate REE ($[La/Yb]_N = 3.86$) and LREE fractionation ($[La/Sm]_N = 3.87$), low HREE fractionation ($[Tb/Yb]_N = 0.61$), and a strong positive Eu anomaly, which could result from apatite or hornblende fractionation, or from crystal accumulation of plagioclase (Taylor et al., 1981; Rollinson, 1993). The Burji granitic gneiss (3 in Fig.1) shows two distinct patterns both in terms of overall REE abundance, fractionation and Eu anomaly. Both patterns are similar to the patterns of the Finchaa granitic gneiss. The Yabello granitic gneiss (1) shows a similar REE pattern to the pattern of subgroup 1 of the Finchaa granitic gneiss (2). The Altuntu granitic gneiss shows two different patterns: one similar to the Finchaa granitic gneiss subgroup 1 pattern and the other showing strong REE fractionation ($[La/Yb]_N=28.82$), moderate LREE fractionation ($[La/Sm]_N = 10.75$), low HREE fractionation ($[Tb/Yb]_N = 1.43$), and a negative Ho anomaly, which is not observed in the other groups.

Adola Granitoids

The Arero granitic gneiss (13 in Fig.1) from the southern part of the Adola granite-gneiss complex (Fig.1b) shows strong overall REE fractionation $[La/Yb]_N=8.68$-16.27), moderate LREE enrichment ($[La/Sm]_N = 3.95$-5.88), flat to slightly depleted HREE patterns

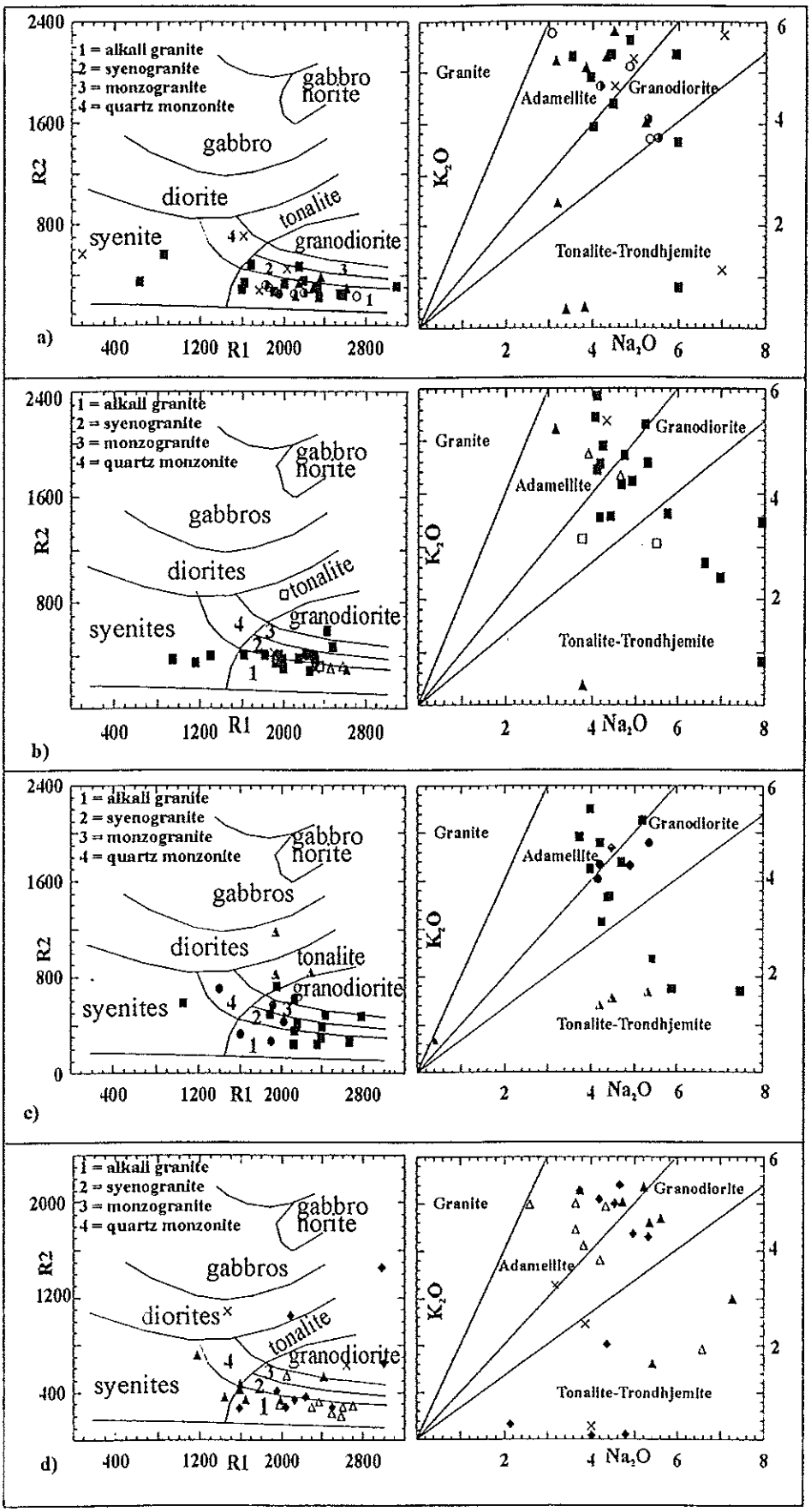

Figure 3: Rock classification diagrams of the gneisses and granitoids of a) Burji-Finchaa, b) Adola, c) Genale-Dolo and d) Moyale-Sololo complexes of southern Ethiopia: R1-R2 : diagram after De La Roche (1978), Na_2O-K_2O diagram after Harpum (1963).

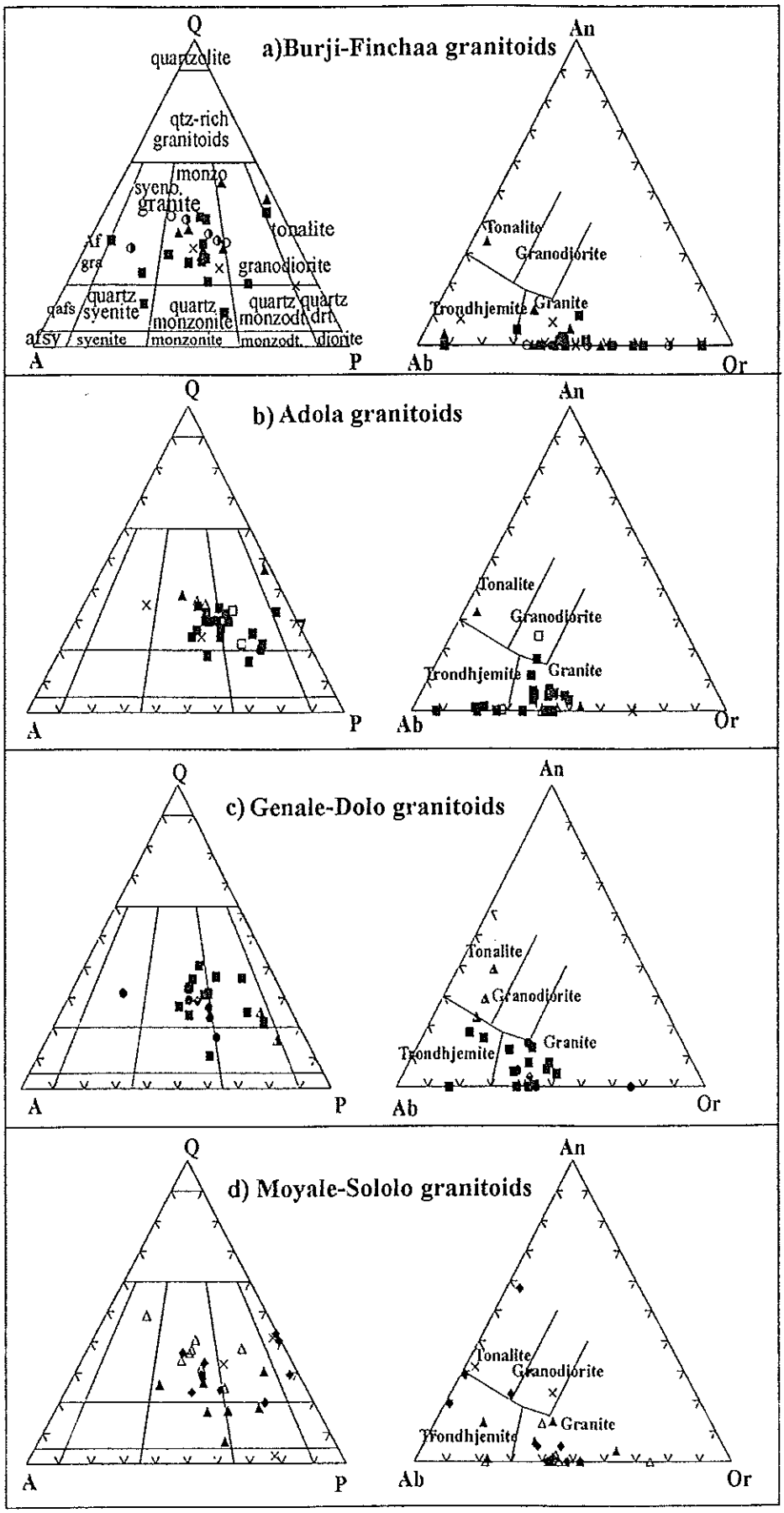

Figure 4: Plutonic rock classification of the granitoids: A-Q-P diagram after Streckeisen (1976), Ab-An-Or diagram after Barker (1979).

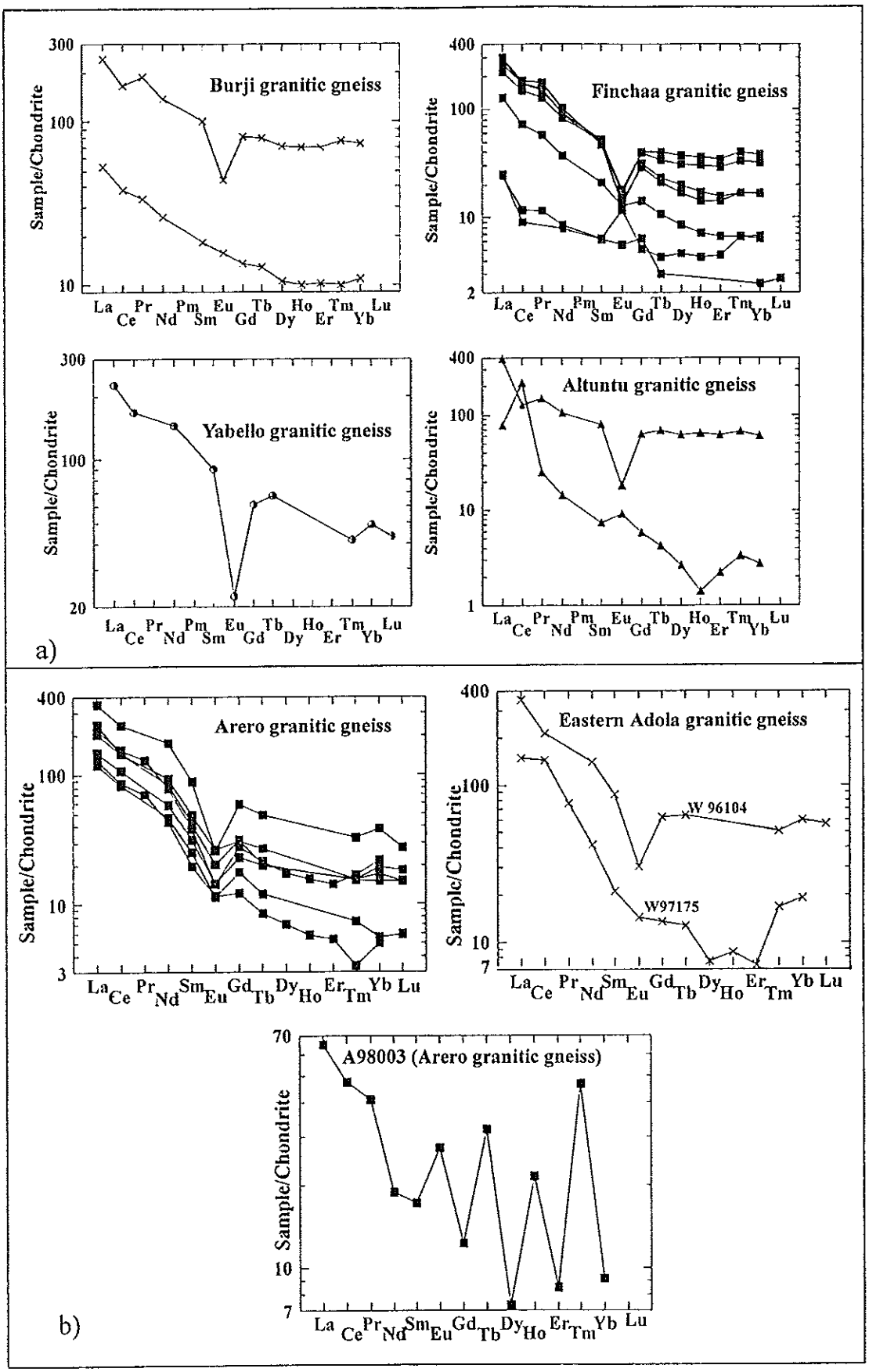

Figure 5: REE plots of chondrite-normalised (CP) and MORB-normalised (MP) data for the granitoids of southern Ethiopia. Chondrite and MORB values from Thompson (1982) and Pearce (1983), respectively.

Figure 5 (contd).

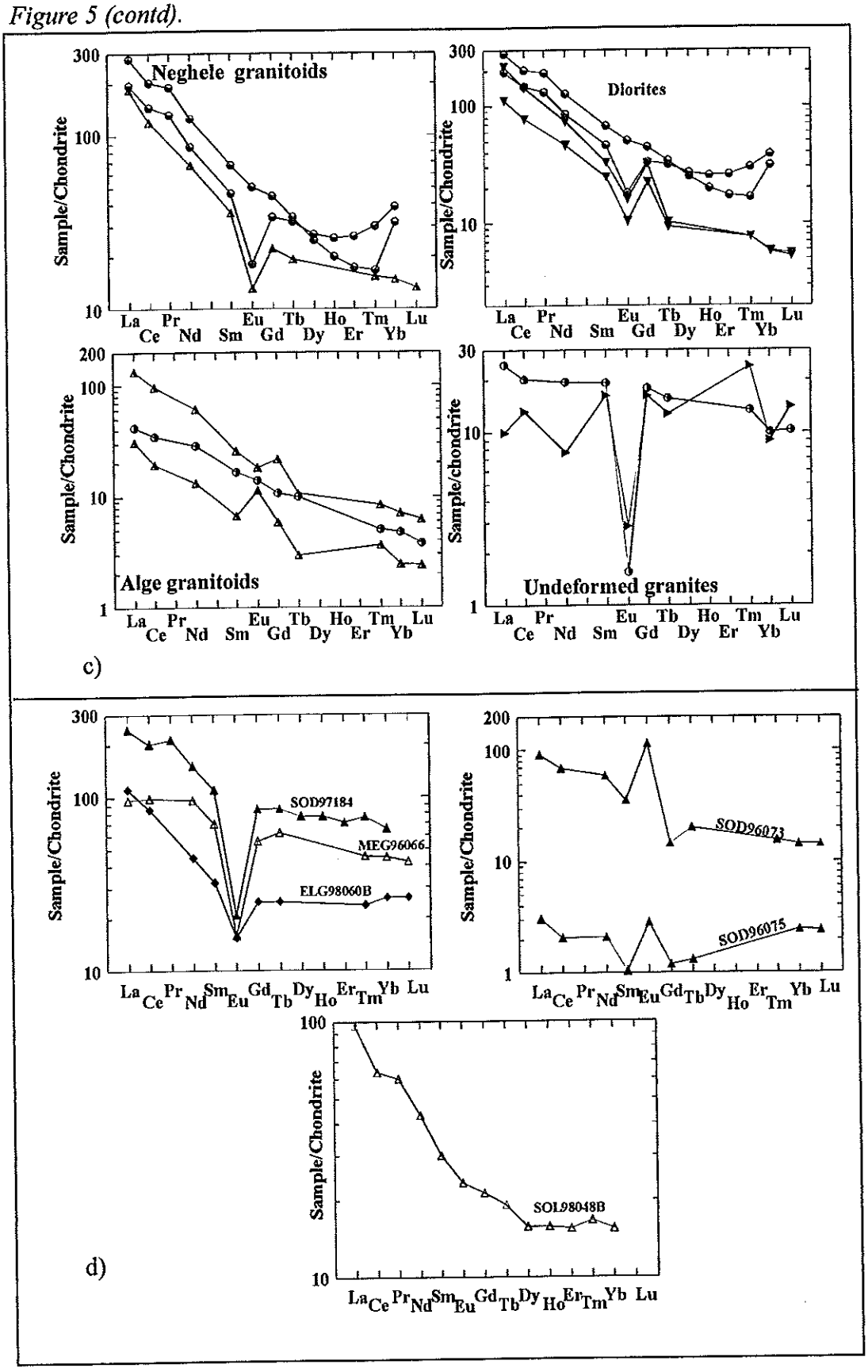

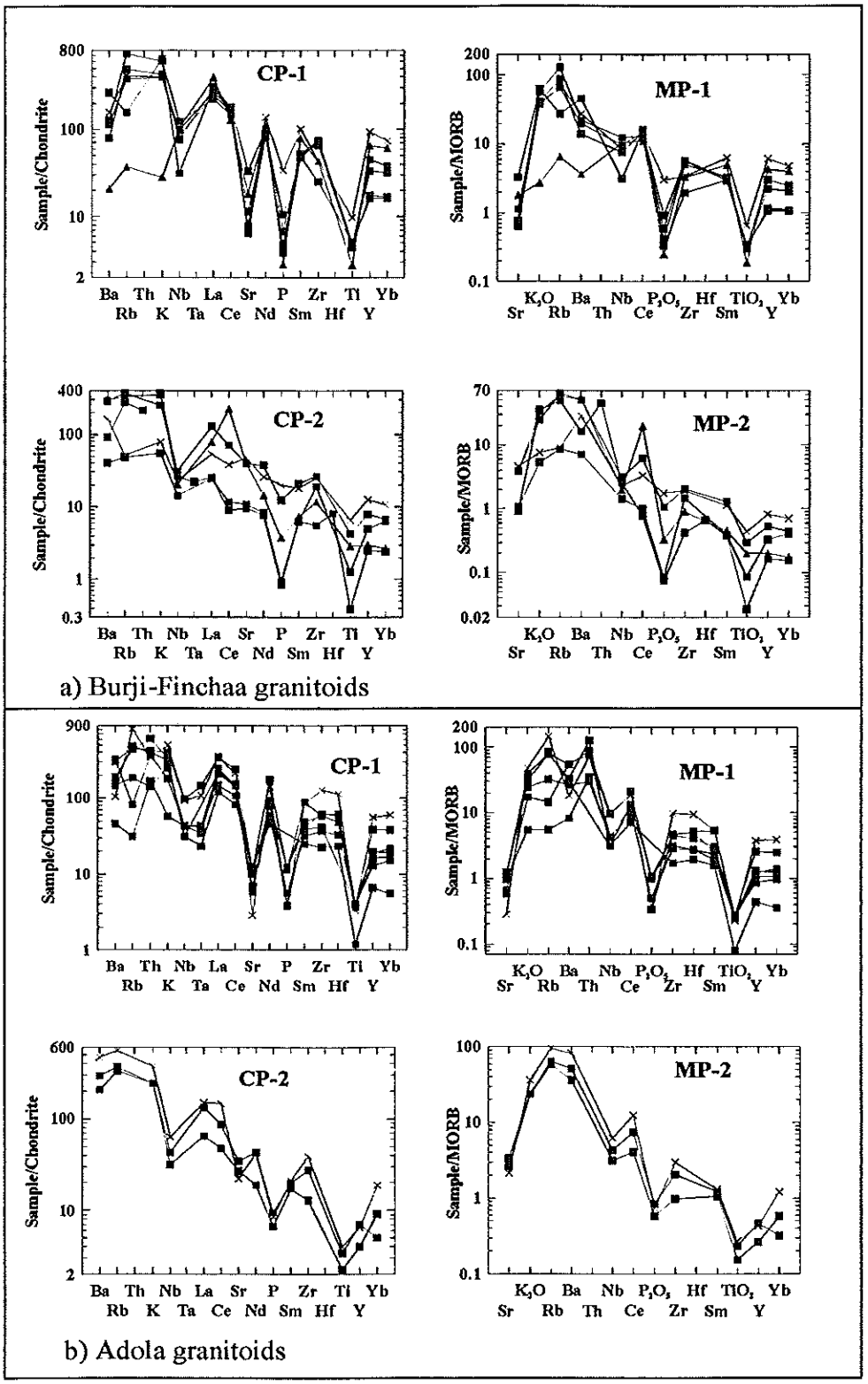

Figure 6: Spider diagrams for the granitoids of southern Ethiopia; CP = chondrite-normalised, MP = MORB-normalised patterns (normalisation data as in Fig.5).

Figure 6 (contd).

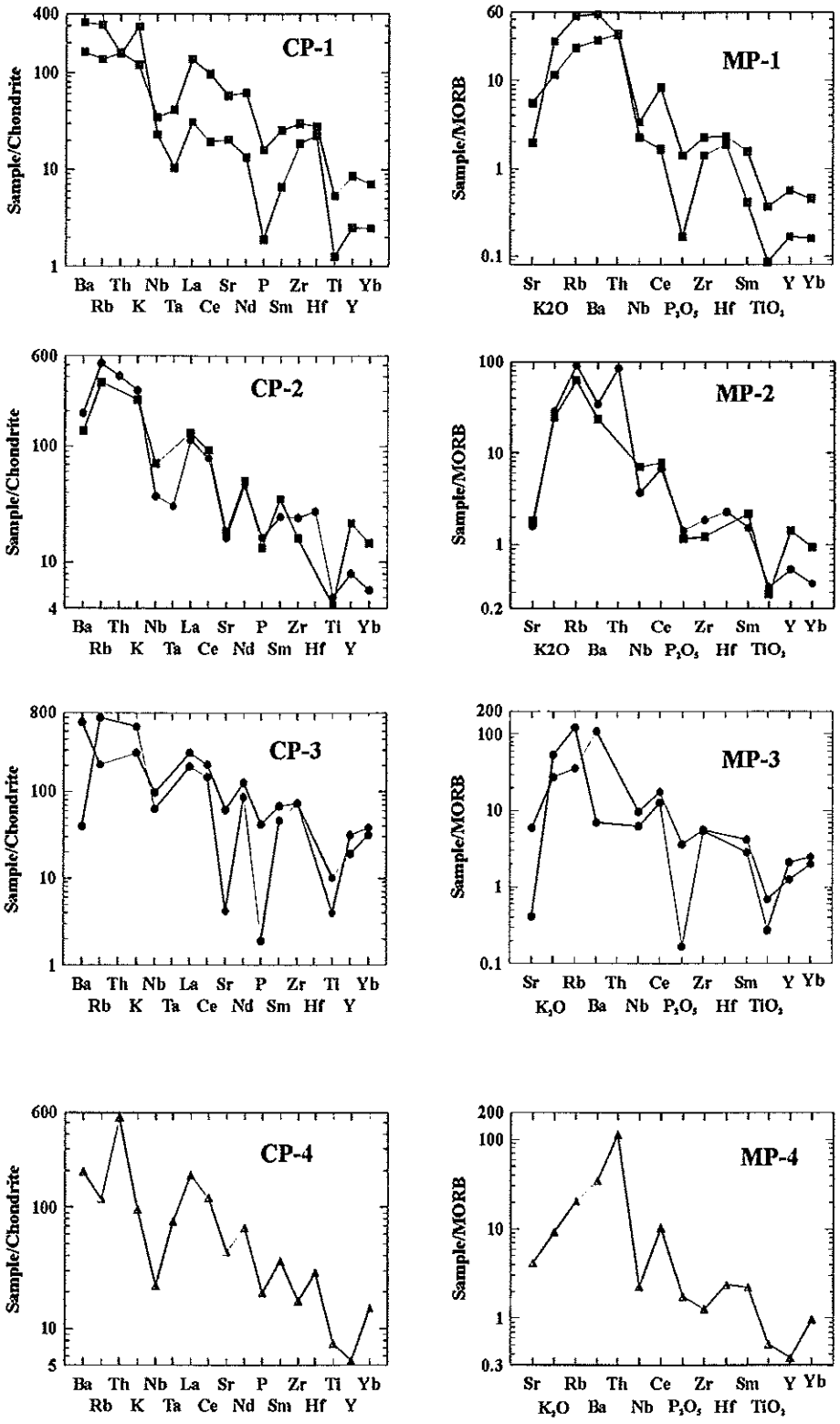

c) Genale-Dolo granitoids

Figure 6 (contd).

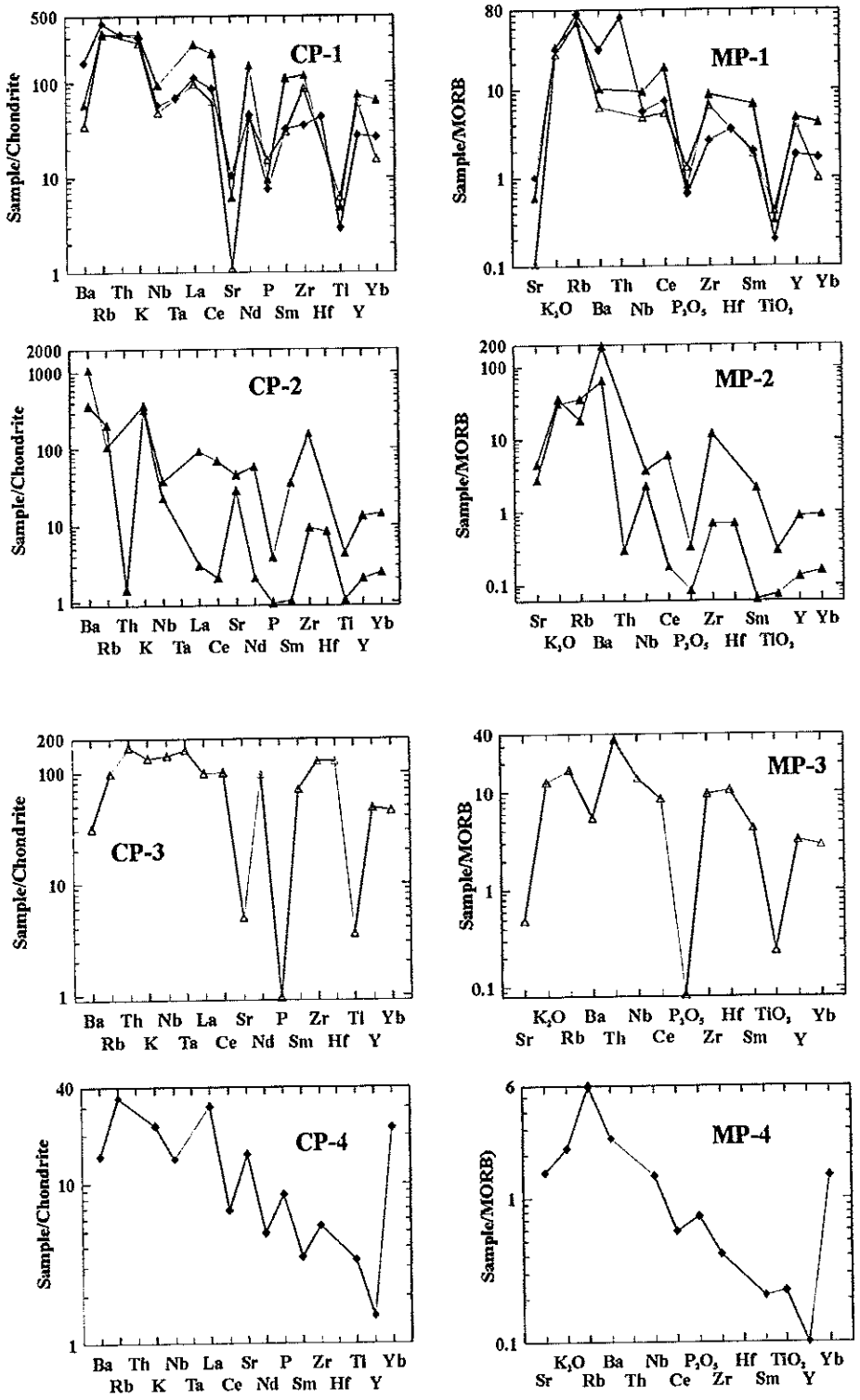

d) Moyale-Sololo granitoids.

($[Gd/Yb]_N$ = 1.34-3.15), and strong negative Eu anomalies. One sample shows an anomalous pattern, especially with respect to its middle and heavy REE pattern (Fig. 5b). The Eastern Adola granitoid (16 in Fig.1) shows variably fractionated REE patterns ($[La/Yb]_N$ = 7.83, 26.2), moderately fractionated LREE ($[La/Sm]_N$ = 7.05, 6.65) and HREE patterns ($[Gd/Yb]_N$ = 2.46, 0.70) (Fig. 5b).

Genale-Dolo Granitoids

The Neghele granitoid gneisses (18 in Fig.1) from the northern part of the Genale-Dolo complex (Fig. 1b) exhibits low-to-moderate overall REE ($[La/Yb]_N$ = 5.05-8.88) and LREE ($[La/Sm]_N$ = 4.21-4.13) fractionation, low HREE fractionation ($[Gd/Yb]_N$ = 0.87-1.43), and a negative Eu anomaly. The pattern for each sample from the Alge granitoid gneisses (20) from the southern part of the Genale-Dolo granite-gneiss complex, are different, although they commonly show strong overall REE fractionation and LREE enrichment. The Wadera (17 in Fig.1) and Melka Guba (21 in Fig.1) megacrystic dioritic gneisses show LREE enriched patterns similar to the other granitoids described above, but differ in terms of the middle REE and HREE. With the exception of the Wadera megacrystic dioritic gneiss, the other dioritic samples in this group show a negative Eu anomaly. The undeformed granites from this complex show lower overall REE abundances, less fractionated patterns, and more pronounced negative Eu anomalies (Fig. 5c) than the deformed granitoid samples.

Moyale-Sololo Granitoids

The granitoids from the Moyale-Sololo granite-gneiss complex (Fig. 1b) show three distinct REE patterns (Fig. 5d). Although the Group-1 samples are taken from three different granitic units on the basis of the field mapping (Fig. 1b), their REE patterns are similar and show moderate fractionation of REE and LREE, low- to -moderately fractionated HREE, and a strong, negative Eu anomaly. Group-2, which represents the Sodigga granitic gneiss (6 in Fig.1), has moderate REE fractionation, flat LREE and HREE patterns, and a strong, positive Eu anomaly. The third group is represented by a single sample (SOL98048B) from the Sololo granitic gneiss (8 in Fig.1) and shows strong LREE fractionation and flat HREE, and has no Eu anomaly.

Spider Diagrams

Spider diagrams of normalised multi-elements data are useful to compare relative concentrations of elements within and between rock suites. They are also used to compare geochemical characteristics of rocks from various geotectonic environments (Wilson, 1989).

There are three popular ways of normalising trace element data for presentation as spider diagrams. The first two compare a rock suite with the composition of the primitive undifferentiated earth, but differ in the rock types (composition of primitive mantle or chondritic meteorites) they are compared with. The third method compares a rock suite with primitive mid-oceanic ridge basalt (MORB). Rollinson (1993) recommended two multi-element diagrams to study igneous rocks: (1) the element order and normalising values of Thompson (1982) to compare with a "mantle source"; and (2) those of Pearce (1983) to compare with the "most abundant volcanic rock" – mid-oceanic ridge basalts (MORB). The latter method is most appropriate for evolved basalts, andesites and crustal

rocks. The MORB and chondrite-normalised multi-element data for the granitoids of the study area are shown in Figure 6.

Burji-Finchaa Granitoids

The multi-element plots for the Burji-Finchaa granitoids tilt to the right, have troughs at the P and Ti positions, and peaks at the Zr and Rb positions. In detail, they can be classified into two groups. Group-1 shows relatively higher MORB-normalised values than Group-2. It also shows a less pronounced trough for Nb and strong peaks for Ce, Zr, Sm and Y (MP-1, Fig. 6a). The chondrite-normalised data give more or less the same patterns, but are characterised by additional peaks for La and Nd (CP-1, Fig. 6a). Group-2 has an overall lower abundance relative to Group-1. It shows a marked trough for Nb, in addition to troughs for Ti and P positions and marked peaks for Ce and Zr, on the MORB-normalised plots (MP-2, Fig. 6a). The chondrite- and MORB-normalised data of Group-2 samples show similar patterns, with the exception of the additional peak for La in the chondrite-normalised data.

Adola Granitoids

The MORB-normalised data patterns for the Adola granitoids are variably tilted to the right (Fig. 6b). These patterns can be classified into two groups based on overall trace element abundance and subtle differences. The MORB-normalised data of Group-1 shows higher overall trace element abundance, troughs for Ba, Nb, P_2O_5 and TiO_2, and peaks for Rb, Th and Ce. It also shows two plateaux formed by Zr-Hf-Sm and Y-Yb (MP-1, Fig. 6b). The chondrite-normalised data for Group-1 shows peaks for La, Ce and Nd and troughs for Sr and Ta, in addition to those peaks and troughs exhibited for the MORB-normalised data (CP-1, Fig. 6b).

Group-2 has lower overall trace element abundance and tilts steeply to the right relative to Group-1 (MP-2 and CP-2, Fig. 6b). Group-2 also lacks the plateaux exhibited by Group-1. The patterns of the MORB-normalised data for Group 2 yields peaks for Rb, Ba, Ce and Zr, and troughs for Nb, P_2O_5 and TiO_2 and the chondrite-normalised data exhibit peaks for La and Ce, Nd and Sm, and troughs for K, Sr, P and Ti.

Genale-Dolo Granitoids

Both the MORB- and chondrite-normalised data for the Genale-Dolo granitoids show patterns that tilt steeply to the right (Fig. 6c). All samples show troughs for Ti and P and varied peaks for Zr, Hf and Sm. The Neghele granitoids (18 in Fig.1) show an overall lower abundance of trace elements relative to the other groups (CP-1, MP-1, Fig. 6c). Their MORB-normalised data show patterns with troughs for Nb, P, and Ti and peaks for Ce and Hf, whereas the chondrite-normalised data show peaks for Th, La, Nd, Sm and Zr. The MORB-normalised patterns of the dioritic gneisses show peaks at the positions of Ti, P, Th, Ce, Y, and Hf or Sm, and troughs for Nb (MP-2, Fig. 6c). The chondrite-normalised patterns (CP-2) of this group show stronger differentiation than those of the other groups in the complex, especially with respect to the HFS elements (Fig. 6c). The chondrite-normalised data for the Alge granitoid gneiss (20 in Fig.1) exhibit patterns similar to those of the Neghele granitoids, but have a positive Y anomaly. The pattern for the MORB-normalised data differs by the presence of a Rb peak (compare CP-3 and MP-3, Fig. 6c). The plot of the chondrite-normalised data for the Bulbul mylonitic diorite (19 in Fig.1)

show a pattern with peaks for Th, La, Nd, Sm and Hf and troughs for Rb, Nb, P, Zr and Y. The plot of the MORB-normalised data shows peaks for Th and Ce, a small plateau defined by Hf and Sm, and troughs for Nb, Zr and Y (MP-4, Fig. 6c). This pattern varies slightly from those of the other diorites (compare CP-2 and MP-2 with CP-4 and MP-4, Fig. 6c).

Moyale-Sololo Granitoids

Overall, the MORB-normalised data for the Moyale-Sololo granitoids show that they are more enriched in LIL elements than average MORB. Group-1 samples, although representing three separately mapped granitoids, commonly show troughs for Sr, P, Ti and Nb and peaks for Rb, Th, Ce, La, Nd, Zr, Sm and Hf, for their chondrite- and MORB-normalised data (MP-1, Fig. 6d). Group-2 represents the Sodigga granitic gneiss (6 in Fig.1) and shows patterns that are tilted more to the right than Group-1 patterns. They show marked troughs for Ti, Th and P positions and peaks for K, Zr, and Hf. The variograms vary from sample to sample with respect to Ce, La, Sr, Nb and Sm (CP-2 and MP-2, Fig. 6d). Group-3 represents the Mega-Hidilola granitic gneiss (7 in Fig.1). Its patterns differ from the other groups in the complex lacking tilt and lower overall trace element concentrations. The plot of the chondrite-normalised data exhibits peaks for Th, K, Nb, and Ta, forming a plateau with a subtle depression for K and Nb. It also shows plateaux defined by Zr-Hf and Y-Nb, peaks for Ce and Nd, and marked troughs for Ti, P and Sr. The MORB-normalised data shows a marked peak for Th, with a steep slope to the right, and peaks for Nb and Ce. The peak for the Nb position is rather anomalous when compared to the other granitoids of the study area. The REE pattern also exhibits a plateau for Zr and Hf (CP-3 and MP-3, Fig. 6d), suggesting that these elements behaved coherently during differentiation or partial melting from a subduction-related magma (e.g., Dostal et al., 1996). Group-4 represents the southern margin of the El-Gof granitic gneiss (6a, Fig. 1b) close to the fault contact of the Moyale-Sololo granite-gneiss complex and the Moyale ophiolitic fold and thrust belt (Yibas, 2000). Its MORB-normalised data shows a pattern with a steep tilt to the right, with a marked peak for Rb and a subtle peak for P_2O_5, and troughs for Y and Ce. The chondrite-normalised data displays selective enrichment and depletion of HFS elements (CP-4 and MP-4, Fig. 6d).

Tectonic Setting

The tectonic setting of granitoids can be inferred from tectonic discrimination diagrams. It must be noted, however, that discrimination diagrams seldom provide unequivocal confirmation of a former tectonic environment; at best, they can be used to suggest an affiliation and they should never be considered of unambiguous value.

Data for the granitoids of the study area are plotted on the Y + Nb vs. Rb tectonic setting discrimination diagram (Fig. 7a) and classify the rocks into volcanic-arc (VAG) and within-plate (WPG) granitoids. Within-plate granitoids can be related to three possible tectonic environments: (1) continental crust of normal thickness; (2) strongly attenuated continental crust; and (3) an anomalous-oceanic-ridge environment. Samples that show WPG characteristics on the Y + Nb vs. Rb diagram fall into the anomalous-oceanic-ridge or attenuated-continental lithosphere field, but not into the WPG field of the Y vs. Nb tectonic discrimination diagram (Fig 7).

The Y + Nb vs. Rb diagram also shows the dominance of volcanic-arc granites over within-plate granites in the study area. Rollinson (1993) pointed out the difficulties of

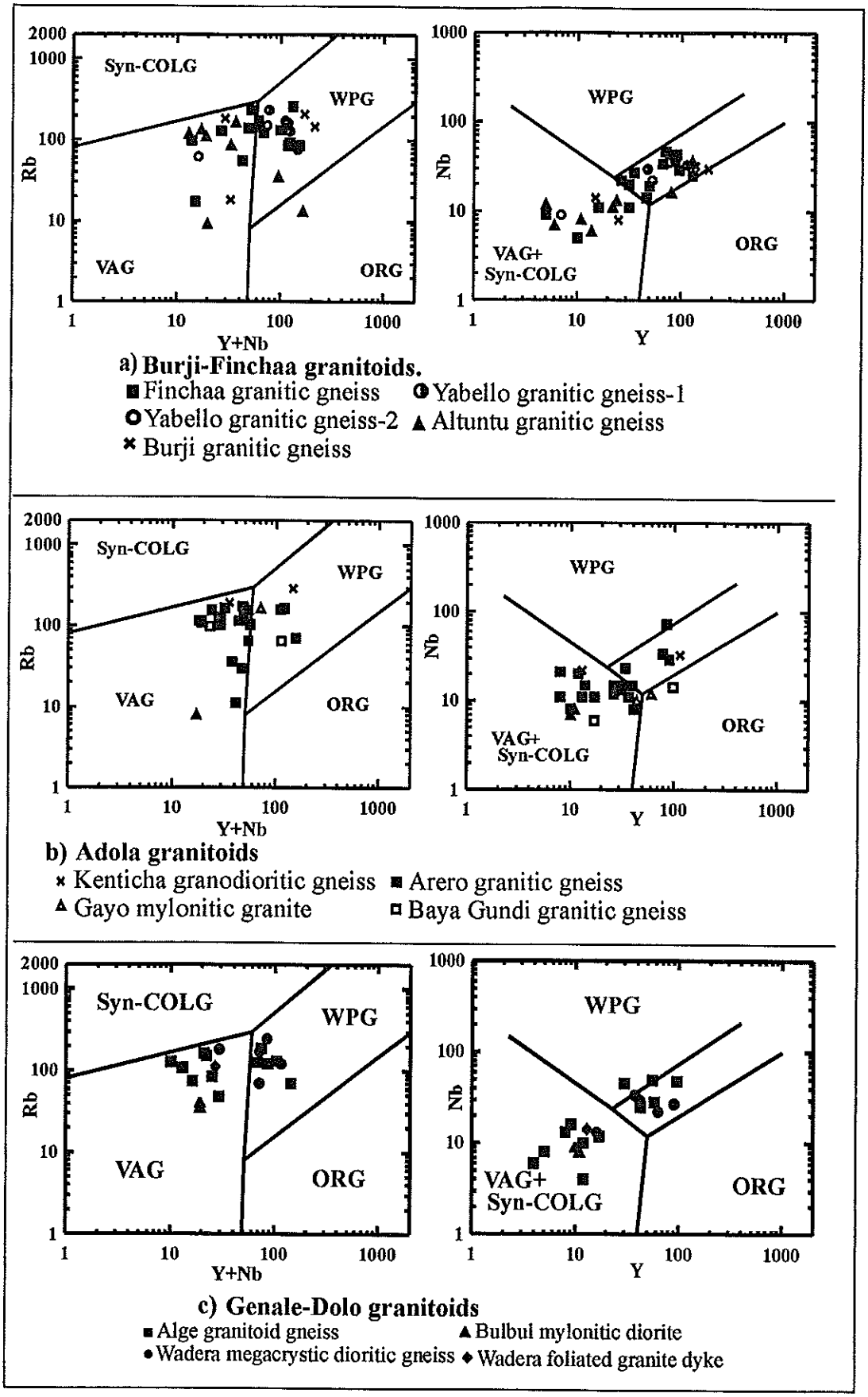

Figure 7: Tectonic discrimination diagrams for the granitoids of southern Ethiopia: Rb - Yb+Nb and Y - Nb diagrams after Pearce et al. (1984); Rb-Ta-Hf diagrams after Harris et al. (1986).

Figure 7 (contd).

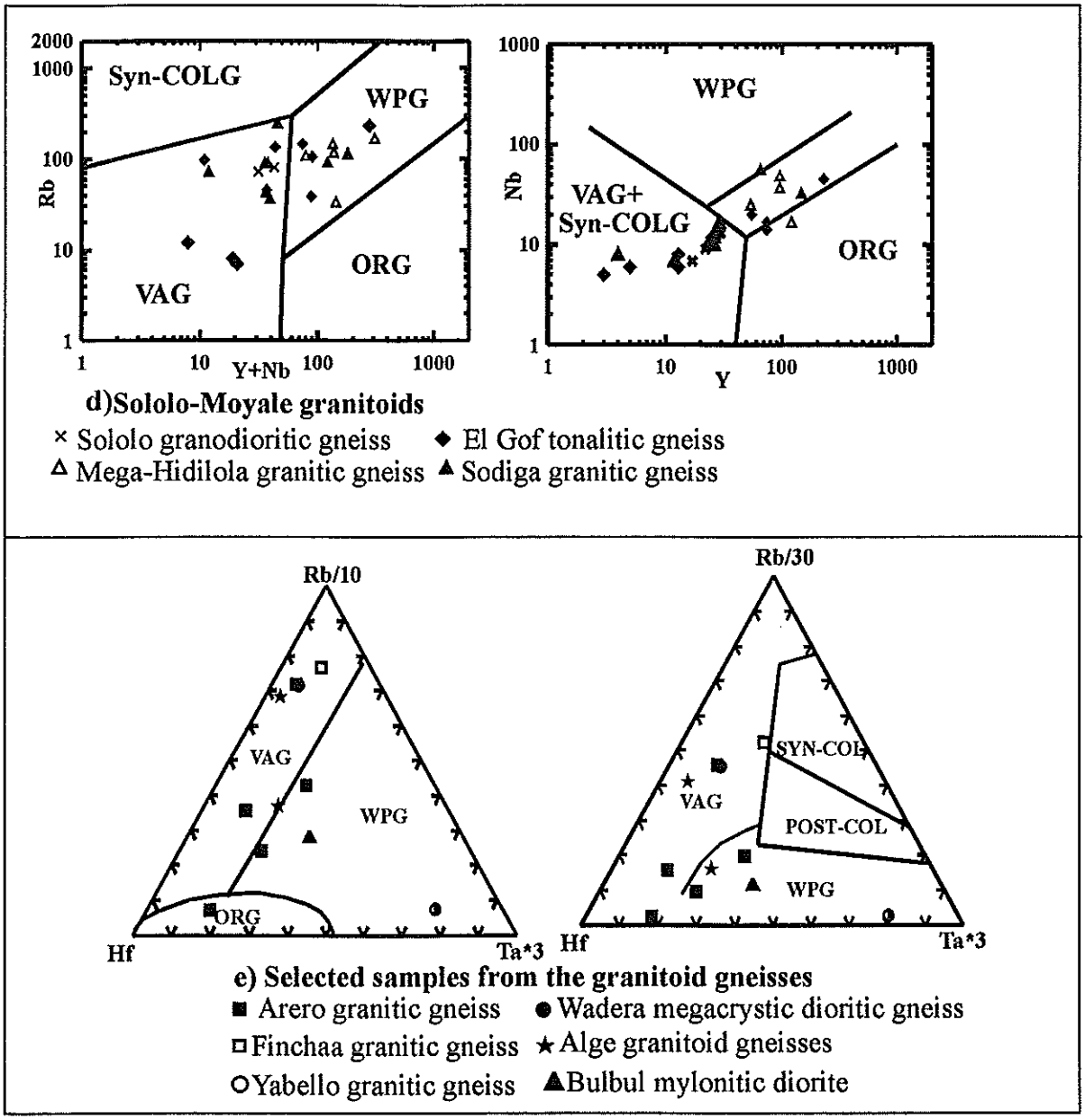

distinguishing post-orogenic granites from volcanic-arc granites and syncollisional granites by using the diagrams of Pearce et al. (1984), but he argued that these types could be distinguished on a Hf-Rb-Ta diagram. This diagram (Fig.7e) demonstrates a scarcity of late- and post-tectonic as well as oceanic-ridge granites amongst the granitoids of the study area.

Granite Classification

As discussed in the previous section, the granitoid gneisses of the study area can be classified into groups associated with two major tectonic settings, viz. the volcanic-arc and within-plate-granitoid settings, whereby volcanic-arc related granitoids appear to be dominant. The samples resembling within-plate granitoids also bear evidence of emplacement into strongly attenuated continental crust, which fits the description of A-type granites.

Chemical classification of rock suites using alumina, alkali element and lime ratios has been found useful in understanding the petrogenesis and tectonic setting of granitoids (Maniar and Piccoli, 1989). For this classification the granitoid samples have been plotted onto the NK/A ($(K_2O + Na_2O)/ Al_2O_3$) vs. A/CNK (Al_2O_3 / K_2O + Na_2O + CaO) diagram (Fig. 8a) after Maniar and Piccoli (1989). Most of the Burji-Finchaa and Adola granitoids have strong peralkaline affinity. The Bulbul mylonitic diorite in the Genale-Dolo granite-gneiss complex shows peraluminous characteristics, whereas the other granitoids in this complex are peralkaline, with a few samples straddling the boundary between the peralkaline and metaluminous fields. The samples from the Moyale-Sololo granitoids are equally divided into peralkaline and metaluminous compositions. The Mega-Hidilola and Sodigga granitoids dominantly show peralkaline affinity, whereas the El Gof granitoids are metaluminous. The Sololo granitic gneiss straddles the boundary of the peraluminous and metaluminous fields.

The majority of data plot in the calcic field on the SiO_2 vs. Na_2O+K_2O diagram of Peackock (1931) (Fig. 8b) similar to Cordilleran and other young fold-belt granites that might contain a component of mantle or subducted oceanic crust (Chappell and White, 1992).

Eby (1992) argued that for high-silica granites, such as the granitoids of the study area, the alkali and CaO contents are not reliable criteria for distinguishing A- from S- and I-type granitoids and recommended the use of the FeO^T/MgO ratio plotted against SiO_2 for more effective discrimination. In this diagram, most samples from the study area fall into the A-type granite field, with a few exceptions from the Adola granitoids, which fall into the I- and S-type granite fields (Fig. 8c). In the HFS elements (Zr + Nb + Ce + Y) vs. $Fe_2O_3{}^T/MgO$ plot after Whalen et al. (1987), most samples plot into the A-type granite field, with a few exceptions that fall into the FG (fractionated) granite field. The samples of the Bulbul mylonitic diorite falls into the OGT (unfractionated M-, I-, and S-type granite) field (Fig. 8d).

A-type Granites

According to Loiselle and Wones (1979), A-type granitoids have high (total) alkali and low CaO contents, and high FeO^T/MgO ratios, and are formed in anorogenic settings along rift zones and within stable continental blocks. Pearce et al. (1984) suggested that A-type granitoids are intruded into within-plate tectonic settings of either continental crust with normal thickness, or into strongly attenuated continental crust. It has been shown here that the granitoids that fall into the within-plate granite field have geochemical affinities with granites emplaced into attenuated continental-crust or with anomalous oceanic-ridge granites (ORG) of strongly attenuated continental lithosphere. Most of these granitoids show A-type granite chemistry.

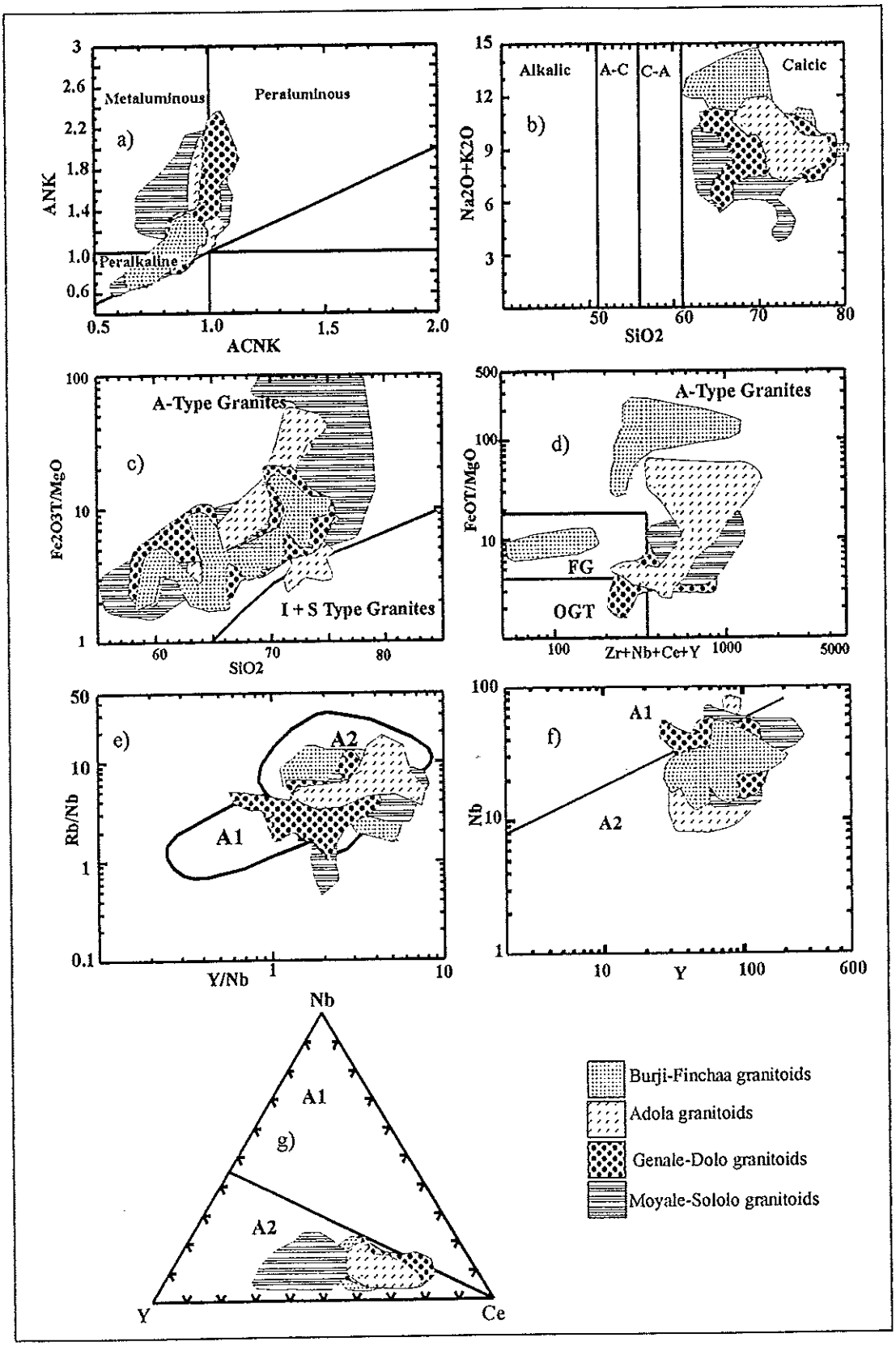

Figure 8: (a) ANK-ACNK (diagram after Maniar and Piccoli, 1989), (b) SiO_2 - (Na_2O+K_2O) (diagram after Peackock, 1931), (c) SiO_2 - $Fe_2O_2^T/MgO$ (after Loiselle and Wones, 1979),(d) Zr+Nb+Ce+Y vs. $Fe_2O_3^T/MgO$ (after Whalen et al., 1987), (e)Y/Nb-Rb/Nb,(f) Y-Nb and (g) Ce-Y-Nb (after Eby, 1992) plots for the granitoids of southern Ethiopia.

According to Eby (1992) a rock suite with A-type granite compositions, with evidence of emplacement into a within-plate tectonic setting on the discrimination diagrams of Pearce et al. (1984), can be further classified into A1- and A2-type granites. Rocks of the A1 group have trace element ratios similar to those of oceanic-island basalts, whereas the A2 group has ratios intermediate between continental crust and island-arc basalts. Most of the A-type granitoids of the study area consistently exhibit A2-type granitic affinity when plotted onto A1-A2 discrimination diagrams (Figs. 8e, f, g). A few exceptions of A1-type are noted, however, from each complex. This constrains the possible tectonic setting and petrogenetic environment for the emplacement of these granitoids to only a few possibilities. The A2-type granitoids include magmas derived from continental crust or underplated crust that has been through a cycle of continent-continent collision or island-arc magmatism (Eby, 1992).

DISCUSSION

Field and petrographic characteristics of the quartzofeldspathic gneisses from southern Ethiopia (Yibas, 2000), coupled with this assessment of their protolith types, indicate that igneous intrusive rocks were the protoliths of most of these gneisses. These granitoids range compositionally from diorites to granites, with monzogranodiorites and granites dominating.

Overall, the REE patterns of the granitoids of the study area appear similar and are comparable to those of many Late Proterozoic granites, such as those from the Northeastern Desert of Egypt (Stern and Gottfried, 1986), the monzogranites of the Eastern Desert of Egypt (Hassanen et al., 1996) and also the younger granites from the Red Sea Hills in Sudan (Klemenic and Poole, 1988). However, the HREE fractionation patterns exhibited by most of the granitoid samples from the study area show similarities with granitoids from continental margin settings, namely intermediate calc-alkaline rocks. Such rocks often show distinct HREE fractionation (i.e., $[Tb/Yb]_N > 1$), which is rare or absent in island-arc granitoids (Thorpe et al., 1976; Dostal et al., 1996).

The spider diagrams for the granitoids of southern Ethiopia indicate enrichment of the most incompatible elements (Rb, Th and Ba) relative to the REEs and HFS elements. The peaks at Zr and Hf positions are related to enrichment of these elements in a parental magma. The troughs for Ti, P and Nb are possible indications of an interplay between parental magma composition and fractional crystallisation processes (e.g., Oyinloye, 1998) in subduction-related environments (see Thompson et al., 1984; Pearce, 1983, for detailed discussion). Most of the patterns also show a regular decrease of the enrichment factor with increasing compatibility of the elements (to the right of the diagram), with strong negative Nb, P, Sr, and Ti anomalies. These features are characteristic of subduction-related magmas, as is the case for other East African Orogen granitoids (Kuster, 1993; Kuster et al., 1993; Kuster and Harms, 1998; Ferre et al., 1998).

The marked peaks for Ce and Sm indicate the presence of minerals such as biotite and K-feldspar and accessories such as sphene, monazite and apatite in these rocks (Rollinson, 1993). Petrographic studies confirm the dominance of K-feldspar among the major rock-forming minerals, with sphene and apatite being the most common accessory minerals in these samples (Yibas, 2000).

The Rb and Sr concentrations and their subtle negative anomalies in the spider diagram patterns depicted by some of the samples are comparable to high-K, calc-alkaline granites and post-collisional granitoids. The weak Sr anomalies suggest that the compositional variation in the granitoids may not be related only to fractional crystallisation mechanisms, but also to assimilation of upper crustal rocks during the ascent of the granitic magma (Kuster and Harms, 1998).

Tectonic discriminant diagrams classify the granitoids of the study area into volcanic-arc granitoids and within-plate granitoids, with dominance of the volcanic-arc granitoids. The within-plate granites are geochemically restricted to the field of attenuated continental crust or anomalous oceanic-ridge granites. Most of the "within-plate" granitoids of the study area are A2-type granitoids. Petrogenetically, the A2-type granitoids include magmas derived from continental crust or underplated crust that has been through a cycle of continent-continent collision or island-arc magmatism (Eby, 1992).

Plots of the geochemical data on granite classification diagrams show that most of these granitoids have metaluminous, peralkaline and calcic affinity. These characteristics suggest similarity of the granitoids of the study area to the Cordilleran and other young fold-belt granites that might contain a component of mantle or subducted oceanic crust (Chappell and White, 1992). Only a few exceptions from the Moyale-Sololo and Adola complexes show peraluminous character. Whereas calc-alkaline granites are considered products of volcanic arc magmatism, alkaline and peralkaline granites are related to within-plate settings. Peraluminous granites are believed to be most commonly the result of continent-continent collision (Pearce et al., 1984).

The granitoids of the Precambrian of southern Ethiopia show gross geochemical similarity with granitoids from western Ethiopia (Kebede et. al., 1999), but differ from those of northern Ethiopia by the absence of with-in plate granitoids and the dominance, in northern Ethiopia, of volcanic-arc I-type granitoids. However, in terms of their relative ages (cp., Taddesse et al., 2000 and Yibas et al., 2000b) they are similar.

Implications for the Geodynamic Evolution of the Precambrian of Southern Ethiopia

Magmatic rocks found in orogenic belts provide a record of the thermal evolution of deep lithospheric roots of a developing orogen. Though the rock eventually sampled may be the end-product of several genetic processes and phases, magmatic suites can be discriminated on the basis of geological, mineralogical, and chemical characteristics (e.g., Barbarin, 1990; Lameyre and Bonin, 1993). Distinct suites associated with the successive episodes of Wilson Cycle processes reflect a relation between geodynamic factors and magma types, which constitutes the basis of the tectonic discrimination schemes currently used (e.g., Pearce et al., 1984; Maniar and Piccoli, 1989).

Following the collision of different plates magmatic suites are located principally in mobile belts. Here reactivated, pre-existing zones of weakness control their emplacement during ensialic deformation. They subsequently change abruptly from typically orogenic syn- to post-collisional suites emplaced during collision, uplift, and subsequent gravitational collapse of the hot and thick crust to transcurrent faulting, peneplanation, and the development of fault-controlled intracontinental molasse basins (Bonin, 1990; Turner et al., 1992).

Table 1. A possible correlation between geochemical affinity and age data for the granitoids of southern Ethiopia (modified from Yibas et al., 2000a)

Granitic Phases/ Ages	Granites	Age (Ma) Zircons	Inferred Tectonic Setting	Reference
Gt7 [550-500 Ma]	Metoarbasebat granite	526±5	WPG (attenuated continental crust).	Yibas et al., 2000b (SHRIMP U-Pb)
	Berguda charnockitic granite	528±8.4 (rim) 538±3 (core)		Gichile, 1991 (U-Pb single zircon evaporation)
	Lega Dima granite	550±18		Worku, 1996 (U-Pb single zircon evaporation)
	Robele granite	554±23		Genzebu et al., 1994 (U-Pb single zircon evaporation)
Gt6 [550-600 Ma]	Wadera granite	576±5	VAG	Yibas et al., 2000b (SHRIMP U-Pb)
	Digati dioritic gneiss	570±5	VAG	Yibas et al., 2000b (SHRIMP U-Pb)
	Wadera megacrystic dioritic gneiss	579±5	WPG (attenuated continental crust)	Yibas et al., 2000b (SHRIMP U-Pb)
Gt5 [700-600 Ma]	Burjiji granite	~602	VAG	Worku, 1996 (U-Pb single zircon evaporation)
	Meleka granodiorite	610±9	VAG	Yibas et al., 2000b (SHRIMP U-Pb)
	Gariboro granite	~646	VAG	Worku, 1996 (U-Pb single zircon evaporation)
	Moyale granodiorite	666+5	VAG	Yibas et al., 2000b (SHRIMP U-Pb)
Gt4 [720-700 Ma]	Finchaa biotite-foliated granite	708±5		Genzebu et al., 1994 (U-Pb single zircon evaporation)
	Yabello granitic gneiss	716±5	WPG (attenuated continental crust).	Teklay et al., 1998 (U-Pb single zircon evaporation)
Gt3 [770-720 Ma]	Alghe granitic-gneiss (western part of the Adola)	722±2		Worku, 1996 (U-Pb single zircon evaporation)
	Sagan basic charnockite	725±5		Teklay et al., 1998 (U-Pb single zircon evaporation)
	Zembaba granitic gneiss	756±6	WPG (attenuated continental crust)	Teklay et al., 1998 (U-Pb single zircon evaporation)
	Sebeto tonalitic gneiss	765±3		Genzebu et al., 1994 (U-Pb single zircon evaporation)
Gt2 [>770 Ma]	Melka Guba megacrystic granodioritic gneiss	778±23	WPG (attenuated continental crust)	Yibas et al., 2000b (SHRIMP U-Pb)
Gt1[>880 Ma]	Bulbul mylonitic diorite	876±7	VAG	Yibas et al., 2000b (SHRIMP U-Pb)

Field relationships, as well as zircon and $^{40}Ar/^{39}Ar$ geochronological data (Yibas, 2000; Yibas et al., 2000b), enabled the classification of the granitoids of southern Ethiopia into 7 magmatic episodes. These include: Gt1 (>880 Ma), Gt2 (>770 Ma), Gt3 (770-720 Ma), Gt4 (720-700 Ma), Gt5 (700-600Ma), Gt6 (600-550 Ma) and Gt7 (550-500 Ma), which cover the time span of the East African Orogen (Yibas, 2000; Yibas et al., 2000b).

Geochemical studies have shown the presence of within-plate and volcanic-arc granitic magmatism in the study area of southern Ethiopia. Correlation of the geochemical interpretation with the age data (Yibas et al., 2000b) indicates a possible alternation of within-plate and volcanic-arc granites with time (Table1). This, in turn, can be used to imply that the granitoid magmatism in southern Ethiopia represents repeated compression and extension during the evolution of the East African Orogen between 900 and 500 Ma ago.

ACKNOWLEDGEMENTS

This paper has resulted from the PhD project by Bisrat Yibas, which benefited from generous financial support from Anglo American Prospecting Services, Johannesburg. Special thanks go to Sharon Farrell of the Geology Department of the University of the Witwatersrand, who conducted the major element chemical analyses. Richard Holdsworth and his group at the Anglo American Research Laboratory (AARL), Johannesburg, are thanked for undertaking the ICP-MS trace element analyses.

REFERENCES

Barker, J., 1979. Trondhjemite: definition, environment, and hypothesis of origin, 1-12. *In*: F. Barker (ed.), *Trondhjemites, Dacites and Related Rocks*. Elsevier, Amsterdam, 659pp.

Barbarin, B., 1990. Granitoids: main petrogenetic classifications in relation to origin and tectonic setting. Spec. Issue, Geol. J., **25**, 227-238.

Bonin, B., 1990. From orogenic to anorogenic settings: evolution of granitoids suites after a major orogenesis. Spec. Issue, Geol. J., **25**, 261-270.

Carl, J.D., 1988. Popple Hill Gneiss as dacite volcanics: a geochemical study of mesosome and leucosome, northwest Adirondacks, New York. Bull. Geol. Soc. Amer., **100**, 841-849.

Chappell, B.W. and White, A.J.R., 1992. I- and S-type granites in the Lachlan Fold Belt. Trans. Royal Soc. Edinburgh, Earth Sciences **83**, 1-26.

De La Roche, H., 1978. La chimie des roches présentée et interprétée d'après la structure de leur facies minèral dans l'espace des variables chimiques: fonctions spécifiques et diagrammes qui s'en déduisent. Application aux roches ignées. Chem. Geol., **21**, 63-87.

Dostal, J., Keppie, J.D., Cousens, B.L. and Murphy, J.B., 1996. 550-800 Ma magmatism in Cape Breton Island (Nova Scotia, Canada): the product of the NW-dipping subduction during the final stage of amalgamation of Gondwana. Precambrian Res.,**76**, 93-113.

Eby, G.N., 1992. Chemical subdivision of the A-type granitoids: petrogenetic and tectonic implications. Geology 20, 641-644.

Ferre, E.C., Cabby, R., Peucat, J.J., Capdevila, Monie, P., 1998. Pan-African, post-collisional, ferro-potassic granite and quartz-monzonite plutons of Eastern Nigeria. Lithos **45**, 255-280.

Genzebu, W., Hassen, N. and Yemane, T., 1994. Geology of the Agere Mariam area. Mem. Ethiopian Inst. Geol. Surv., Addis Ababa, **8**, 23pp.

Gichile, S., 1991. *Structure, metamorphism and tectonic setting of a gneissic terrane, the Sagan-Aflata area, southern Ethiopia.* M.Sc thesis (unpubl.), Univ. Ottawa, Canada, 224pp.

Hanson, G.N., 1978. The application of trace elements to the petrogenesis of igneous rocks of granitic composition. Earth Planet. Sci. Lett., **38**, 26-43.

Harpum, J. R., 1963. Petrographic classification of granitic rocks in Tanganyika by partial chemical analyses. Record, Geol. Surv. Tanganyika, **10**, 80-88.

Harris, N.B. W., Pearce, J. A. and Tindle, A.G., 1986. Geochemical characteristics of collision zone magmatism. *In*: M.P. Coward and A. C. Ries (eds.), *Collision Tectonics.* Blackwell Scientific Publications, London. Spec. Publ. Geol. Soc. Lond., **19**, 67-81.

Hassanen, M. A., Said, A.E. and Mohamed, F.H., 1996. Geochemistry and petrogenesis of Pan-African I-type granitoids at Gabal Igla Ahmar, Eastern Desert, Egypt. J. Afr. Earth Sci., **22**, 29-42.

Irvine, T.R. and Baragar, W.R.A., 1971. A guide to the chemical classification of the common volcanic rocks. Can. J. Earth Sci., **8**, 523-548.

Kebede, T., Koeberl, C. and Koller, F., 1999. Geology, geochemistry and petrogenesis of intrusive rocks of the Wallagga area, western Ethiopia. J. Afr. Earth Sci., **29**, 715-734.

Key, R. M., Charsley, T. J., Hackman, B. D., Wilkinson, A. F. and Rundle, C.C., 1989. Superimposed upper Proterozoic collision-controlled orogenesis in the Mozambique Belt of Kenya. Precambrian Res., **44**, 197-225.

Klemenic, P. M. and Poole, S., 1988. The geology and geochemistry of upper Proterozoic granitoids from the Red Sea Hill. J. Geol. Soc. Lond., **145**, 635-643.

Koeberl, C., 1993. Instrumental neutron activation analysis of geochemical and cosmochemical samples: a fast and proven method for small sample analysis. J. Radioanal. Nucl. Chem., **168**, 47-60.

Kuster, D., 1993. Geochemistry and petrogenesis of Permo-Jurassic oversaturated alkaline complexes of northern Kordofan, central Sudan, 197-201. *In*: U. Thorweihe and W. Schandelmeier (eds.), *Proceedings of the International Conference on Geoscientific Research in Northeast Africa.* Berlin, Germany.

Kuster, D. and Harms, U., 1998. Post-collisional potassic granitoids from the southern and northwestern parts of the Late Neoproterozoic East African orogen: a review. Lithos, **45**, 177-195.

Kuster, D., Hengst, M. and Pilot, J., 1993. Evolution of Pan-African granitoid magmatism along the southwestern Nakasib suture, Red Sea Hills, Sudan, 111-116. *In*: U. Thorweihe and H. Schandelmeier (eds.), *Proceedings of the International Conference on Geoscientific Research in Northeast Africa*. Berlin, Germany.

Lameyre, J. and Bonin, B., 1993. Granites in the main plutonic series, 3-17. *In*: J. Didier and B. Barbarin (eds.), *Enclaves and Granite Petrology. Developments in Petrology 13*, Chapman & Hall, London.

Loiselle, M.C. and Wones, D. R., 1979. Characteristic and origin of anorogenic granites. Abstracts with Programs, Geol. Soc. Amer., **11**, p. 468.

Maniar, P.D. and Piccoli, P.M., 1989. Tectonic discrimination of granitoids. Bull. Geol. Soc. Amer., **101**, 635-643.

Munyanyiwa, H., Richard, E.H., Blenkinsop, T. G. and Treloar, P.J., 1997. Geochemistry of amphibolites and quartzofeldspathic rocks in the Pan-African Zambezi Belt, northwest Zimbabwe: evidence for bimodal magmatism in a continental rift setting. Precambrian Res., **81**, 179-196.

Nesbitt, H.W. and Young, G.M., 1982. Early Proterozoic climates and plate motions inferred from major element chemistry of lutites. Nature, **299**, 715-717.

Nesbitt, H.W. and Young, G.M., 1984. Prediction of some weathering trends of plutonic and volcanic rocks based upon thermodynamic and kinetic considerations. Geochim. Cosmochim. Acta , **48**, 1523-1534.

Nesbitt, H.W. and Young, G.M., 1989. Formation and diagenesis of weathering profiles. J. Geol., **97**, 129-147.

Oyinloye, A. O., 1998. Geology, geochemistry and origin of the banded gneisses and granite in the basement complex of the Ilesha area, southwestern Nigeria. J. Afr. Earth Sci., **26**, 633-641.

Peackock, M. A., 1931. Classification of igneous rock series. J. Geol., **39**, 54-67.

Pearce, J. A., 1983. Role of the sub-continental lithosphere in magma genesis at active continental margins, 230-249. *In*: C. J. Hawkesworth and M. J. Norry, (eds.), *Continental Basalts and Mantle Xenoliths*. Shiva, Nantwich.

Pearce, J. A., Harris, N.B.W. and Tindle A.G., 1984. Trace element discrimination diagrams for the tectonic interpretation of granitic rocks. J. Petrol., **25**, 956-983.

Reimold W. U., Koeberl, C. and Bishop, J., 1994. Roter Kamm impact crater: geochemistry of basement rocks and breccias. Geochim. Cosmochim. Acta **58**, 2689-2710.

Rollinson, H.R., 1993. *Using Geochemical Data: Evaluation, Presentation, Interpretation.* Wiley, New York, 351pp.

Shackleton, R.M., 1997. The final collision zone between East and West Gondwana: where is it? J. Afr. Earth Sci., **23**, 289-310.

Shaw, D.M., 1972. The origin of the Apsley Gneiss, Ontario. Can. J. Earth Sci., **9**, 18-35.

Stern, R.J. and Gottfried, D., 1986. Petrogenesis of a late Precambrian (570-600Ma) bimodal suite in northeast Africa. Contrib. Mineral. Petrol., **92**, 492-501.

Streckeisen, A., 1976. To each plutonic rock its proper name. Earth Sci. Rev., **12**, 1-33.

Taddesse, T., Hoshino, M., Suzuki, K. and Iizumi, S., 2000. Sm-Nd, Rb-Sr and Th-U-Pb zircon ages of syn- and post-tectonic granitoids from Axum area of northern Ethiopia. J. Afr. Earth Sci., **30**, 313-327.

Teklay, M., Kröner, A., Mezger, K. and Oberhänsli, R., 1998. Geochemistry, Pb-Pb single zircon ages and Nd-Sr isotope composition of Precambrian rocks from southern and eastern Ethiopia: implications for crustal evolution in East Africa. J. Afr. Earth Sci., **26**, 207-227.

Thompson, R. N., 1982. Magmatism of the British Tertiary volcanic province. Scot. J. Geol., **18**, 49-107.

Thompson, R. N., Morison, M. A., Hendry, G. L. and Parry, S. J., 1984. An assessment of the relative roles of crust and mantle in magma genesis: an elemental approach. Phil. Trans. R. Soc., **A310**, 549-590.

Thorpe, R. S., Potts, P.J. and Francis, P.W., 1976. Rare earth data and petrogenesis of andesites from the north Chilean Andes. Contrib. Mineral. Petrol., **54**, 65-78.

Turner, S., Sandiford, M. and Foden, J., 1992. Some geodynamic and compositional constraints on 'post-orogenic magmatism. Geology, **20**, 931-934.

Van de Kamp, P.C. and Beakhouse, G. P., 1979. Paragneisses in the Pakwash Lake area, English River Gneiss Belt, Northwest Ontario. Can. J. Earth Sci., **16**, 175-1763.

Whalen, J.B., Currie, KL. and Chappell, B.W., 1987. A-type granites: geochemical characteristics, discrimination and petrogenesis. Contrib. Mineral. Petrol., **95**, 407-419.

Wilson, M., 1989. *Igneous Petrogenesis: a Global Tectonic Approach.* Unwin Hyman, London, 466pp.

Worku, H., 1996. *Geodynamic development of the Adola Belt (southern Ethiopia) in the Neoproterozoic and its control on gold mineralisation.* Ph.D thesis (unpubl.), Berlin Technical University, Germany, 156pp.

Worku, H. and Schandelmeier, H., 1996. Tectonic evolution of the Neoproterozoic Adola Belt of southern Ethiopia: evidence for Wilson Cycle process and implications for oblique plate collision. Precambrian Res., 77, 179-210.

Yibas, B., 2000. *The Precambrian geology, tectonic evolution, and controls of gold mineralisations in southern Ethiopia.* Ph.D thesis (unpubl.), Univ. Witwatersrand, Johannesburg, 448 pp.

Yibas, B., Reimold, W. U. and Anhaeusser, C. R., 2000a. The geology of the Precambrian of southern Ethiopia: I - the tectonostratigraphic record. Inform. Circ. Econ. Geol. Res. Inst., Univ. Witwatersrand, Johannesburg , **344**, 21 pp.

Yibas, B., Reimold, W.U., Armstrong, R., Phillips, D. and Koeberl, C., 2000b. The geology of the Precambrian of southern Ethiopia: II - U-Pb single zircon SHRIMP and laser argon dating of granitoids. Inform. Circ. Econ. Geol. Res. Inst., Univ. Witwatersrand, Johannesburg 345, 31 pp.

oOo